JCTC Journal of Chemical Theory and Computation

Frozen Gaussian Wavepacket Study of the Ground State of the He Atom

Ling Wang and Eli Pollak*

Chemical Physics Department, Weizmann Institute of Science, 76100 Rehovoth, Israel

Received November 9, 2006

Abstract: The Rayleigh−Ritz functional is used in conjunction with an *approximate* time evolution to improve ab initio estimates of ground-state energies. The improvement is due in part to the introduction of a novel variational "normalization function" for the approximate propagator. An additional variational parameter was introduced in the form of a constant shift energy of the Hamiltonian. The approximate propagator used was the frozen Gaussian propagator; however, the trajectories evolved on the coherent-state averaged Hamiltonian (Q representation). For Coulombic forces, this removes the singularity, easing the computation. An additional variational parameter was the width parameter used for the coherent states appearing in the frozen Gaussian propagator. Using an initial combination of nine Gaussian functions for He, with an initial energy of −2.5115 au, the variational method, with a very short time interval of integration, led to an improved energy of −2.81 ± 0.04 au.

I. Introduction

The quantum mechanics of the He atom in its lowest electronic state are well-understood. One can employ any number of standard ab initio chemistry packages to create a Gaussian basis set which is large enough to accurately diagonalize the Hamiltonian of the He atom and provide accurate estimates of the energies of the lowest eigenstates. Alternatively, one may employ quantum Monte Carlo (MC) simulation methods.[1] This does not mean that the solution is trivial. The He atom has two electrons whose motions are strongly coupled to each other and the He nucleus. For this reason, the He atom is a "good" testing ground for different approaches to the solution of the quantum dynamics of complex systems.

The real-time quantum dynamics of complex systems can at least in principle shed light also on structure. The simplest route is to Fourier-transform the time-dependent overlap of a wavefunction with itself. In principle, the transform will give a series of peaks whose energies are the eigenenergies of the system under study. The Fourier transform however provides accurate estimates only if the time interval used is very long. It must be much larger than $2\pi\hbar/\Delta E$, where ΔE is the level spacing between adjacent levels. It is notoriously difficult to compute numerically the long time quantum dynamics of complex systems. This led to the invention of the filter diagonalization method (FDM)[2,3] where the characteristic time needed is $2\pi\hbar/\bar{E}$, where $\bar{E}$ is the local average level energy. This time scale is much shorter than the time scale arising from the level spacing. The central object in the FDM is the overlap function of an initial state $|\Psi\rangle$ with its time evolved form:

$$c(t) = \langle\Psi|\hat{K}(t)|\Psi\rangle \tag{1.1}$$

where $\hat{K}(t) = \exp(-iHt/\hbar)$. Harmonic inversion is then used to represent the correlation function in terms of the eigenvalues of the Hamiltonian. The FDM method is not foolproof; as noted by Mandelshtam,[3] "the degree of convergence will always be a delicate issue".

Using a related approach, we have recently shown[4] how one can employ the Rayleigh−Ritz functional

$$E[\Psi] = \frac{\langle\Psi|H|\Psi\rangle}{\langle\Psi|\Psi\rangle} \geq E_0 \tag{1.2}$$

(where E_0 denotes the exact ground-state energy) together with time propagation to obtain improved estimates of the ground-state energy. By using as a trial function the linear combination of $|\Psi\rangle + \hat{K}(t)|\Psi\rangle$, the functional becomes time-dependent, and one can use the time as a variational parameter to improve upon the initial estimate for the energy. Here too, the characteristic time needed is on the order of $2\pi\hbar/\bar{E}$, much shorter than the Fourier time.

The time-dependent methods are, though, predicated on the solution of the real-time quantum dynamics. Even for

* Corresponding author e-mail: eli.pollak@weizmann.ac.il.

10.1021/ct600332v CCC: $37.00
Published on Web 02/16/2007

short times, this is not easy. Although significant progress has been made during the past decade,[5−16] the challenge of creating a general methodology remains formidable. The difficulty has created a flurry of more approximate quantum propagation methods of which perhaps the semiclassical initial value representation (SCIVR) and its variants is one of the more promising approaches.[17−19,21−26] The SCIVR methodology has a long history; here, we note two complementary approximations. Heller[18] invented the frozen Gaussian propagation, which was then improved upon by Herman and co-workers,[19,20] who introduced a prefactor to the frozen Gaussian. Although the prefactor significantly improves the quality of the approximation, there is a heavy price to pay; instead of having to solve $2N + 1$ equations of motion (where N is the number of degrees of freedom and the extra equation is for the action), one has to solve an additional $4N^2$ equations of motion to obtain the time-dependent monodromy matrix elements. The difficulty is that, without the prefactor, the frozen Gaussian approximation rapidly loses normalization.[27]

Interestingly, if one wants to employ the time as a variational parameter within the Rayleigh−Ritz functional, one really does not need the exact real-time propagation. Any approximate propagator $\hat{K}_0(t)$ will still give a time-varying functional, and if the energy is lower than that obtained from the initial wavefunction, then one will have improved upon the original choice. In this paper, we report results for the time-dependent variational functional using a variationally optimized frozen Gaussian SCIVR for the propagator. To overcome the loss of normalization which would render the method useless, we introduce an additional variational time-dependent function into the linear combination. We find that a very short time propagation reduces the energy from -2.5115 to -2.81 ± 0.04 au (the ground-state energy is -2.9038 au). However, due to the fact that the frozen Gaussian propagation is effected through a Monte Carlo procedure, the statistical error is rather large, and it is expensive to reduce it to acceptable chemical accuracy.

In section II, we describe the variational method used to propagate the initial wavefunction. Numerical results are presented in section III; we end in section IV with a discussion of the results and their implication for future studies using approximate propagation methods.

II. Theory

A. Time-Dependent Variational Theory. We assume that some initial normalized wavefunction $|\Psi\rangle$ has been chosen. The estimate for the ground-state energy associated with the wavefunction is

$$E_\Psi = \langle\Psi|\hat{H}|\Psi\rangle \tag{2.1}$$

The wavefunction is time-evolved under the action of some approximate propagator, such that

$$|\Psi_0(t)\rangle = \hat{K}_0(t)|\Psi\rangle \tag{2.2}$$

In our previous work,[4] we chose the linear combination $|\phi(t)\rangle = |\Psi\rangle + K(t)|\Psi\rangle$ as the time-dependent wavefunction to be inserted into the Rayleigh−Ritz upper-bound expression for the ground-state energy. In this paper, we will not use the exact propagator but the frozen Gaussian propagator (see also below), which rapidly loses normalization. This would suggest that one should compute the normalization function

$$N_\Psi(t) = \langle\Psi_0(t)|\Psi_0(t)\rangle \tag{2.3}$$

and renormalize the propagator to $\hat{K}_0(t)/\sqrt{N_\Psi(t)}$.

Apart from normalization, there exist other identities. For example, $E_\Psi = \langle\Psi|\hat{K}^\dagger(t)\,\hat{H}\,\hat{K}(t)|\Psi\rangle$ [where $\hat{K}(t) = \mathrm{e}^{-i\hat{H}t}$ is the exact quantum propagator] since the exact propagator commutes with the Hamiltonian. One could thus equally well renormalize the approximate propagator to $\hat{K}_0(t)\sqrt{E_\Psi(0)/E_\Psi(t)}$ where

$$E_\Psi(t) = \frac{\langle\Psi_0(t)|\hat{H}|\Psi_0(t)\rangle}{\langle\Psi_0(t)|\Psi_0(t)\rangle} \equiv \frac{H_\Psi(t)}{N_\Psi(t)} \tag{2.4}$$

This suggests that the best result will be obtained by renormalizing the approximate propagator by an unknown real function $f(t)$ to be determined variationally.

Additional freedom and better results may be obtained by demanding that the function be complex. However, the same result may be obtained in a more physically transparent and numerically stable way by shifting the Hamiltonian by an arbitrary constant energy ϵ. This shifts the ground-state energy by the same constant value. The approximate propagator then becomes $\mathrm{e}^{-i\epsilon t/\hbar}\,\hat{K}_0(t)$ so that the trial time-dependent wavefunction will be

$$|\phi(t)\rangle = |\Psi\rangle + f(t)\,\mathrm{e}^{-i\epsilon t}\,\hat{K}_0(t)|\Psi\rangle \tag{2.5}$$

The time-dependent Rayleigh−Ritz functional for the ground-state energy, obtained by subtracting out the constant shift energy, then becomes eq 2.6 (see Chart 1). This functional

Chart 1

$$E(t) = \frac{\langle\Psi|\hat{H}|\Psi\rangle + fe^{-i\epsilon t}\langle\Psi|\hat{H}\hat{K}_0(t)|\Psi\rangle + fe^{i\epsilon t}\langle\Psi|\hat{K}_0^\dagger(t)\hat{H}|\Psi\rangle + f^2\langle\Psi|\hat{K}_0^\dagger(t)\hat{H}\hat{K}_0(t)|\Psi\rangle}{1 + fe^{-i\epsilon t}\langle\Psi|\hat{K}_0(t)|\Psi\rangle + fe^{i\epsilon t}\langle\Psi|\hat{K}_0^\dagger(t)|\Psi\rangle + f^2\langle\Psi|\hat{K}_0^\dagger(t)\hat{K}_0(t)|\Psi\rangle} \geq E_0 \tag{2.6}$$

Chart 2

$$f(\varepsilon,t) = \frac{-(H_\Psi(t) - N_\Psi(t)E_\Psi)}{H_\Psi(t)S_\Psi(t,\varepsilon) - N_\Psi(t)h_\Psi(t,\varepsilon)} \pm \frac{\sqrt{(H_\Psi(t) - N_\Psi(t)E_\Psi)^2 - (h_\Psi(t,\varepsilon) - E_\Psi S_\Psi(t,\varepsilon))(H_\Psi(t)S_\Psi(t,\varepsilon) - N_\Psi(t)h_\Psi(t,\varepsilon))}}{H_\Psi(t)S_\Psi(t,\varepsilon) - N_\Psi(t)h_\Psi(t,\varepsilon)} \tag{2.7}$$

now depends on four unknowns, the time, the width parameter of the coherent states (see below), the shift energy, and the yet to be determined function $f(t)$.

Variation of the energy with respect to the function $f(t)$ leads to a quadratic equation whose two solutions are given in eq 2.7 (see Chart 2), where we used the additional notation

$$h_\Psi(t,\epsilon) = e^{i\epsilon t/\hbar}\langle\Psi|\hat{H}\,\hat{K}_0|\Psi\rangle + \text{cc} \tag{2.8}$$

$$S_\Psi(t,\epsilon) = e^{-i\epsilon t/\hbar}\langle\Psi|\hat{K}_0|\Psi\rangle + \text{cc} \tag{2.9}$$

The dependence of the variational energy $E(t)$ on the shift energy ϵ is known analytically. For each fixed time, one varies the shift energy to determine the time-dependent minimal energy. One then finds the minimal energy with respect to the remaining time variable. This process may then be repeated for different width parameters to obtain the best minimum.

B. Frozen Gaussian Propagation. The coordinate representation of a coherent state in one dimension is

$$\langle x|g(p,q)\rangle = \left(\frac{\Gamma}{\pi}\right)^{1/4}\exp\left[-\frac{\Gamma}{2}(x-q)^2 + \frac{i}{\hbar}p(x-q)\right] \tag{2.10}$$

where p and q are respectively the coherent-state momentum and coordinate and Γ is the width parameter. The He atom has two electrons; in Cartesian space, these correspond to six degrees of freedom, three for each electron. We will thus employ a multidimensional coherent state defined as a product of the six one-dimensional functions. Because of symmetry, the width parameters for all functions are taken to be identical.

The Hamiltonian of the He atom (in atomic units so that $\hbar = 1$, $m_e = 1$, etc.) is

$$\hat{H} = \sum_{i=1}^{6}\frac{\hat{p}_i^{\,2}}{2} - \frac{2}{\hat{r}_1} - \frac{2}{\hat{r}_2} + \frac{1}{\hat{r}_{12}} \tag{2.11}$$

with $\hat{r}_i^2 = \hat{x}_i^2 + \hat{y}_i^2 + \hat{z}_i^2$, $i = 1$ and 2, and $\hat{r}_{12}^2 = (\hat{r}_1 - \hat{r}_2)^2$. The coherent-state averaged Hamiltonian (also known as the Q representation of the Hamiltonian[28]) is then readily found to be[29]

$$H(\mathbf{p},\mathbf{q}) \equiv \langle g(\mathbf{p},\mathbf{q})|\hat{H}|g(\mathbf{p},\mathbf{q})\rangle = \sum_{i=1}^{6}\frac{p_i^{\,2}}{2} + \frac{3}{2}\Gamma + V_\Gamma(r_1,r_2,r_{12}) \tag{2.12}$$

where the coherent-state averaged potential is

$$V_\Gamma(r_1,r_2,r_{12}) \equiv -2\frac{\text{erf}(\sqrt{\Gamma}r_1)}{r_1} - 2\frac{\text{erf}(\sqrt{\Gamma}r_2)}{r_2} + \frac{\text{erf}\left(\sqrt{\frac{\Gamma}{2}}r_{12}\right)}{r_{12}} \tag{2.13}$$

All classical trajectories $\mathbf{p}_t$ and $\mathbf{q}_t$ will be propagated using Hamilton's equations as derived from the Q-representation Hamiltonian. Note that in this representation the singularity associated with the Coulomb potential at the origin is removed.

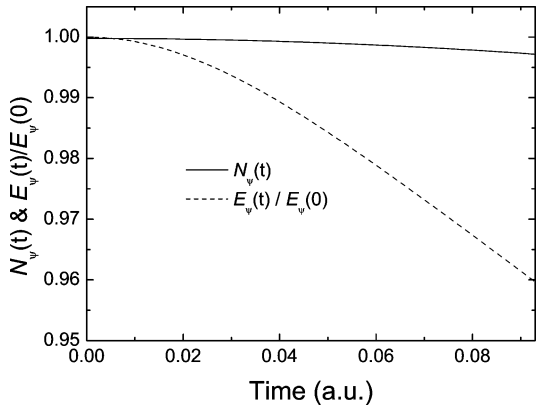

Figure 1. Normalization $N_\Psi(t)$ and the normalized energy function $E_\Psi(t)/E_\Psi(0)$ plotted as a function of time. The reduced energy function varies more rapidly than the normalization. Note that the decrease of the reduced energy function implies an *increase* in the energy $E_\Psi(t)$ with time, since $E_\Psi(0) < 0$.

The frozen Gaussian propagator is defined as

$$\hat{K}_0(t) = \int\frac{d\mathbf{p}\,d\mathbf{q}}{(2\pi)^6}\exp[i\,W(\mathbf{p},\mathbf{q};t)]|g(\mathbf{p}_t,\mathbf{q}_t)\rangle\langle g(\mathbf{p},\mathbf{q})| \tag{2.14}$$

and the classical action is

$$W(\mathbf{p},\mathbf{q};t) = \int_0^t dt'\left[\sum_{i=1}^{6}\frac{p_i^{\,2}(t')}{2} - \frac{3}{2}\Gamma - V_\Gamma(r_1,r_2,r_{12};t')\right] \tag{2.15}$$

The energy functional is then obtained by evaluating the various integrals, using a Monte Carlo methodology which takes advantage of the Gaussian structure of the coherent states as described in the Appendix.

III. Numerical Results

To simulate a typical result obtained from a Gaussian program, we first optimized with the Gaussian program the energy for a single-electron wavefunction consisting of three Gaussians. Our initial wavefunction was thus chosen to be the normalized product of the two single one-electron wavefunctions:

$$\langle x|\Psi\rangle = \sum_{i=1}^{3}\sum_{j=1}^{3}a_i a_j\exp(-b_i r_1^{\,2})\exp(-b_j r_2^{\,2}) \tag{3.1}$$

The parameters are $a_1 = 0.074\,877$, $a_2 = 0.259\,881$, $a_3 = 0.171\,081$, $b_1 = 6.362\,42$, $b_2 = 1.158\,23$, and $b_3 = 0.313\,650$. The initial energy $\langle\Psi|H|\Psi\rangle = -2.5115$ au is much higher than the exact ground-state energy of the He atom -2.9038 au. This choice of wavefunction mimics to some extent the complexity of ab initio Gaussian wavefunctions. It contains nine terms and thus implies that the various overlap functions include 81 integrals. Even if one can evaluate accurately with Monte Carlo methods a single integral, it is not clear a priori that one could obtain reasonable accuracy for the sum on the order of 10^2 terms whose sign may change.

The Monte Carlo methodology used to evaluate the various integrals is described in Appendix A. In the numerical results presented in Figures 1−3, we used 10^8 Monte Carlo sample points and a time step of $\Delta t = 0.003$ au for integrating the

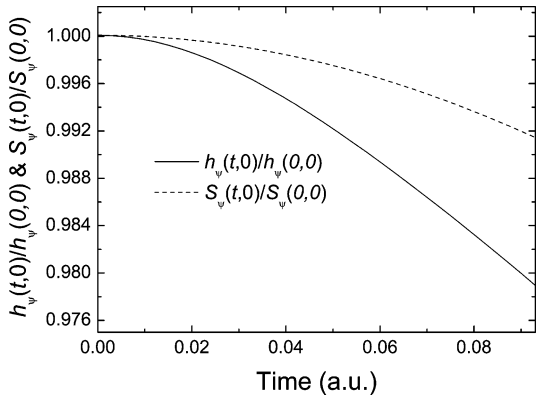

Figure 2. Time-dependent normalized energy overlap function and normalized overlap function vs time for the He atom. These functions are needed to estimate the Rayleigh−Ritz expression. Note the smoothness of the functions. For further details, see the text.

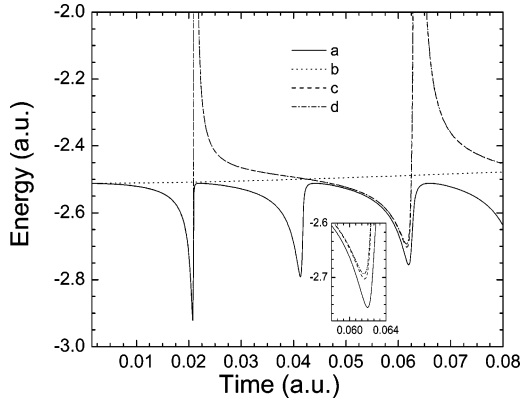

Figure 3. Time-dependent energy as a function of time for fixed values of the shift energy ϵ. The solid line (a) shows the time-dependent energy obtained by the quadratic eq 2.7 optimization of $f(\epsilon,t)$ at the fixed scaling energy $\epsilon = -148$ au. The dotted line (b) is obtained by setting $\epsilon = 0$ and $f(\epsilon,t) = 1$. The dashed line (c) shows the energy obtained after renormalizing the frozen Gaussian propagator with the time-dependent normalization $[\hat{K}_0(t)/\sqrt{N_\Psi(t)}]$, while the dashed dotted line (d) shows the result obtained after renormalization of the propagator with the time-dependent energy $[\hat{K}_0(t)\sqrt{E_\Psi(0)/E_\Psi(t)}]$. Both lines c and d are also obtained at the fixed scaling energy $\epsilon = -148$ au. The inset shows the improvement obtained by using the variational solution for the function $f(\epsilon,t)$.

classical equations of motion. The width parameter Γ appearing in the coherent state was varied so as to minimize the energy; the optimal value we found was $\Gamma = 0.5$ (au).

In Figure 1, we plot the normalization function $N_\Psi(t)$ (eq 2.3) as a function of time. For the exact quantum propagator, this function is a constant equal to unity. We also plot (dashed line) the normalized energy function $E_\Psi(t)/E_\Psi(0)$ (see eq 2.4) as a function of the time. Here too, for the exact quantum propagator, this function equals unity at all times. Interestingly, the variation of the normalization is slower than the variation in time of the energy. Therefore, the normalized energy function $E_\Psi(t)/N_\Psi(t)$ increases monotonically in time. The normalized time-dependent energy does not lead to any improvement in the estimate of the ground-state energy.

The computation of the normalization function $N_\Psi(t)$ and the energy function $E_\Psi(t)$ is substantially more expensive than the computation of the overlap functions. Here, one has a product of two propagators, and so it is necessary to perform a double integration over the system phase space. The integrand is much more oscillatory, and so the accuracy of the results is lower. However, the Monte Carlo sample used was sufficiently large to ensure that the plots shown in the figure are as accurate as the width of the line.

The functions $h_\Psi(t,0)/h_\Psi(0,0)$ and $S_\Psi(t,0)/S_\Psi(0,0)$ are plotted in Figure 2. It is significant to note that also these functions vary smoothly with the energy. It is therefore not difficult to solve the quadratic equation for the variational function $f(\epsilon,t)$. As noted earlier, employing the function within a variational context is the optimal strategy with respect to different renormalizations of the frozen Gaussian propagator. In Figure 3, we plot the time-dependent energy for four different scenarios. The solid line shows the time-dependent energy obtained by the quadratic eq 2.7 optimization of $f(\epsilon,t)$ at the fixed scaling energy $\epsilon = -148$ au. The dotted line is obtained by setting $\epsilon = 0$ and $f(\epsilon,t) = 1$. As already noted above, this gives a monotonically increasing function of the energy. Using the frozen Gaussian propagation without any further optimization does not lead to any improvement relative to the initial result for the ground-state energy. The dashed line shows the energy obtained after renormalizing the frozen Gaussian propagator with the time-dependent normalization $[\hat{K}_0(t)/\sqrt{N_\Psi(t)}]$, while the dashed dotted line shows the result obtained after renormalization of the propagator with the time-dependent energy $[\hat{K}_0(t)\sqrt{E_\Psi(0)/E_\Psi(t)}]$. Both lines are obtained at the fixed scaling energy $\epsilon = -148$ au. Both of these results are similar to each other and to the optimal result; however, the optimal result does provide a significant improvement in the minima obtained as a function of time.

Although it would seem that the first minimum shown in the figure comes very close to the exact ground-state energy, this is misleading. The minimal energy found at $t = 0.021$ au is $E_{\min} = -2.92 \pm 0.73$. The reason for the huge error bar comes from the fact that, at the minimum, the denominator of the energy functional eq 2.6 almost vanishes. Even though each term in the denominator separately is evaluated with an accuracy of at least 4×10^{-4}, the close cancellation of all terms leaves us with an unacceptable statistical error. Reducing the error to acceptable limits turned out to be too costly.

The results shown in Figure 3 are, though, instructive. They show that the lowest minimum is obtained at very early times. Only a small amount of time propagation seems to go a long way in obtaining an improved result. With this in mind, as well as the observed smoothness of the various functions, we repeated the computation, using a much larger time step in the integration of the classical equations of motion and only the three times $t = 0.021$, 0.0315, and 0.042 au. The Monte Carlo sample used for $t = 0.021$ was 1.305×10^{10} MC steps; for $t = 0.0315$ it was 6.48×10^9 MC steps and for $t = 0.042$, 3.5×10^9 MC steps. For the three times $t = 0.021$, 0.0315, and 0.042 au, we used 1, 2, and 2 integration time steps, respectively. This computation led to

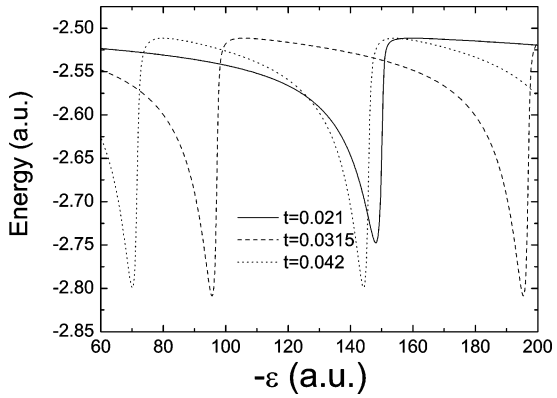

Figure 4. Energy as a function of the energy shift ϵ at fixed times. The solid line shows the energy functional as a function of the energy shift at the fixed time $t = 0.021$ au. The minimum energy $E_{min} = -2.748 \pm 0.035$ au is found at $\epsilon = -148$. The dashed lined shows the same but at the fixed time $t = 0.0315$ au. Here, the minimum energy $E_{min} = -2.809 \pm 0.036$ au is found at $\epsilon = -95.2$ au. The dotted line gives the results for $t = 0.042$ au where the minimum energy $E_{min} = -2.799 \pm 0.026$ au is found for $\epsilon = -70$ au.

a sufficiently small error, as shown below. The solid line in Figure 4 shows the energy functional as a function of the energy shift ϵ at the fixed time $t = 0.021$ au. The minimum energy $E_{min} = -2.748 \pm 0.035$ au is found at the shift energy $\epsilon = -148$. The dashed line shows the same but at the fixed time $t = 0.0315$ au. Here, the minimum energy $E_{min} = -2.809 \pm 0.036$ au is found at $\epsilon = -95.2$ au. Finally, the dotted line is for $t = 0.042$ au, where the minimum energy $E_{min} = -2.799 \pm 0.026$ au is found for $\epsilon = -70$ au. We thus conclude that only a very short time propagation is needed to significantly improve the original estimate of the energy from -2.51 to -2.81 au. These results should be compared with the exact ground-state energy of He which is -2.9038 au.

IV. Discussion

This paper presents some new elements in the time-dependent variational determination of ground-state energies. The Rayleigh−Ritz functional was used in conjunction with an *approximate* time evolution. We showed that one can significantly improve the ground-state energy, even when the time propagation is not precise. A second new element was the introduction of the variational "normalization function" $f(\epsilon,t)$ for the approximate propagator. The use of this variational function compensated for the lack of normalization in the approximate propagator. The third element was the introduction of the shift energy, or equivalently allowing the "normalization function" to be complex. Numerically, we found that more stable results were obtained by introducing the shift energy and varying it.

The model studied was the He atom. The approximate propagator was the frozen Gaussian propagator, where we also introduced a novel element; namely, the trajectories were propagated on the Q-representation Hamiltonian rather than the bare Hamiltonian as was usually done thus far. As in the coupled coherent-states method,[29] this removes the singularity in the potential, making it easier to propagate the classical trajectories.

The methodology led to a significant improvement relative to the initial energy. Only very short time propagation was needed to improve the accuracy of the ground state by roughly 75%. The computation itself was not trivial. Not only was it necessary to perform 12 fold integrals, the final results came from a summation of close to 100 terms. This points out the complexity of carrying out even the simplest SCIVR type of computation for strongly coupled systems such as the two electrons of the He atom. It is this complexity which necessitated averaging over $\sim 10^9$ samples, making the computation very costly. Even with this extensive computation, the error bars in the final energy were large on a chemical scale; an error of 0.02 au in energy is an error of ~ 13 kcal/mol. Reducing the error by an additional factor of 10 would imply increasing the sample size to 10^{11}.

The conclusion from all of this is that perhaps the time-dependent variational method will ultimately turn out to be useful; however, the SCIVR route, even for the short times needed, is not. Present variational and diffusion Monte Carlo methods converge with chemical accuracy to the ground state of He.[30,31] The purpose of this paper was not to present a method which can already compete with such well-known and well-tested methods. Rather, we demonstrated the kind of insight and quality of answer that one may obtain from a very different approach, namely, real-time propagation coupled with the variational theorem. It remains to be seen in future work whether perhaps basis set approaches such as the coupled coherent-states method or the multiconfiguration time-dependent Hartree method can lead to better and more accurate results.

Acknowledgment. This work has been supported by grants of the U.S.−Israel Binational Science Foundation, the Israel Science Foundation, the Donors of the American Chemical Society Petroleum Research Fund, and the German−Israel Foundation for Basic Research.

Appendix A: Monte Carlo Sampling

A Monte Carlo sampling is needed to carry out the integration over the 12-dimensional phase space of the two electrons. In any of the integrals, one always has matrix elements of the projection of the initial wavefunction onto the coherent states $\langle g(\mathbf{p},\mathbf{q})|\Psi\rangle$. The wavefunction is composed of nine terms, three for each electron, so that this overlap has the following form:

$$\langle g(\mathbf{p},\mathbf{q})|\Psi\rangle = \left(\frac{\Gamma}{\pi}\right)^{3/2} \sum_{i=1}^{3}\sum_{j=1}^{3} a_i a_j \left(\frac{\pi}{\Gamma/2+b_i}\right)^{3/2}\left(\frac{\pi}{\Gamma/2+b_j}\right)^{3/2} \prod_{k=1}^{3} \exp\left[-\frac{\Gamma b_i (q_1^{\,k})^2}{2(\Gamma/2+b_i)} + \frac{i b_i p_1^{\,k} q_1^{\,k}}{(\Gamma/2+b_i)\hbar} - \frac{(p_1^{\,k})^2}{4\hbar^2(\Gamma/2+b_i)}\right] \prod_{k=1}^{3} \exp\left[-\frac{\Gamma b_j (q_2^{\,k})^2}{2(\Gamma/2+b_j)} + \frac{i b_j p_2^{\,k} q_2^{\,k}}{(\Gamma/2+b_j)\hbar} - \frac{(p_2^{\,k})^2}{4\hbar^2(\Gamma/2+b_j)}\right] \quad \text{(A.1)}$$

where the superscript k denotes the three Cartesian directions x, y, and z and the subscripts 1 and 2 denote the phase-space variables for electrons 1 and 2, respectively. Since the wavefunction $|\Psi\rangle$ is composed of Gaussian functions, one naturally obtains the Gaussian weightings in phase space which come from the overlap. These Gaussian functions

$$\prod_{k=1}^{3} \exp\left[-\frac{\Gamma b_i (q_1^{\,k})^2}{2(\Gamma/2 + b_i)} - \frac{(p_1^{\,k})^2}{4\hbar^2(\Gamma/2 + b_i)}\right]$$

and

$$\prod_{k=1}^{3} \exp\left[-\frac{\Gamma b_j (q_2^{\,k})^2}{2(\Gamma/2 + b_j)} - \frac{(p_2^{\,k})^2}{4\hbar^2(\Gamma/2 + b_j)}\right]$$

are then used to implement the Box−Muller method for Gaussian probability distributions, replacing the respective coordinates and momenta by random variables according to

$$q_1^{\,k} = \sqrt{\frac{\Gamma/2 + b_i}{\Gamma b_i/2}[-\ln(1-\zeta)]}\cos(2\pi\eta)$$

$$p_1^{\,k} = \sqrt{4\hbar^2(\Gamma/2 + b_i)[-\ln(1-\zeta)]}\sin(2\pi\eta)$$

$$q_2^{\,k} = \sqrt{\frac{\Gamma/2 + b_j}{\Gamma b_j/2}[-\ln(1-\zeta)]}\cos(2\pi\eta)$$

$$p_2^{\,k} = \sqrt{4\hbar^2(\Gamma/2 + b_j)[-\ln(1-\zeta)]}\sin(2\pi\eta) \quad \text{(A.2)}$$

where, $k = 1-3$, and ζ and η are random numbers varying in the interval (0,1).

References

(1) Schmidt, K. E.; Ceperley, D. M. In *The Monte Carlo Method in Condensed Matter Physics*; Springer: Berlin, 1992; p 203.

(2) Wall, M. R.; Neuhauser, D. *J. Chem. Phys.* **1995**, *102*, 8011.

(3) Mandelshtam, V. A. *Proc. Nucl. Magn. Reson. Spectrosc.* **2001**, *38*, 159.

(4) Saltzer, M.; Pollak, E. *J. Chem. Theory Comput.* **2005**, *1*, 439.

(5) Topaler, M.; Makri, N. *J. Chem. Phys.* **1994**, *101*, 7500.

(6) Topaler, M.; Makri, N. *J. Phys. Chem.* **1996**, *100*, 4430.

(7) Stockburger, J.; Mak, C. H. *J. Chem. Phys.* **1999**, *110*, 11.

(8) Stockburger, J.; Grabert, H. *Phys. Rev. Lett.* **2002**, *88*, 170407.

(9) Shalashilin, D. V.; Child, M. S. *J. Chem. Phys.* **2000**, *113*, 10028.

(10) Shalashilin, D. V.; Child, M. S.; Clary, D. C. *J. Chem. Phys.* **2004**, *120*, 5608.

(11) Burant, J. C.; Batista, V. S. *J. Chem. Phys.* **2002**, *116*, 2748.

(12) Beck, M. H.; Jaeckle, A.; Worth, G. A.; Meyer, H.-D.; Kuehn, O. *Phys. Rep.* **2000**, *324*, 1.

(13) Wang, H.; Thoss, M. *J. Chem. Phys.* **2003**, *119*, 1289.

(14) Worth, G. A.; Robb, M. A.; Burghardt, I. *Faraday Discuss.* **2004**, *127*, 307.

(15) Burghardt I. In *Quantum Dynamics of Complex Systems*; Micha, D. A., Burghardt, I., Eds.; Springer: New York, 2006; Springer Series in Chemical Physics, Vol. 83, p 135.

(16) Kuleff, A. I.; Breidbach, J.; Cederbaum, L. S. *J. Chem. Phys.* **2005**, *123*, 044111.

(17) Miller, W. H. *J. Chem. Phys.* **1970**, *53*, 3578.

(18) Heller, E. J. *J. Chem. Phys.* **1981**, *75*, 2923.

(19) Herman, M. F.; Kluk, E. *Chem. Phys.* **1984**, *91*, 27.

(20) Kluk, E.; Herman, M. F.; Davis, H. L. *J. Chem. Phys.* **1986**, *84*, 326.

(21) Grossmann, F. *Comments At. Mol. Phys.* **1999**, *34*, 141.

(22) Tannor, D. J.; Garaschuk, S. *Annu. Rev. Phys. Chem.* **2000**, *51*, 553.

(23) Baranger, M.; de Aguiar, M. A. M.; Keck, F.; Korsch, H. J.; Schellhaas, B. *J. Phys. A: Math. Gen.* **2001**, *34*, 7227.

(24) Miller, W. H. *J. Phys. Chem. A* **2001**, *105*, 2942.

(25) Kay, K. G. *Annu. Rev. Phys. Chem.* **2005**, *56*, 255.

(26) Pollak, E. In *Quantum Dynamics of Complex Systems*; Micha, D. A., Burghardt, I., Eds.; Springer: New York, 2006; Springer Series in Chemical Physics, Vol. 83, p 259.

(27) Harabati, C.; Rost, J. M.; Miller, W. H. *J. Chem. Phys.* **2004**, *120*, 26.

(28) Martin-Fierro, E.; Gomez Llorente, J. M. *Chem. Phys.* **2006**, *322*, 13.

(29) Shalashilin, D. V.; Child, M. S. *J. Chem. Phys.* **2005**, *122*, 224108.

(30) Kole, J. S.; De Raedt, H. *Phys. Rev. E: Stat., Nonlinear, Soft Matter Phys.* **2001**, *64*, 016704.

(31) Ma, A.; Drummond, N. D.; Towler, M. D.; Needs, R. J. *Phys. Rev. E: Stat., Nonlinear, Soft Matter Phys.* **2005**, *71*, 066704.

CT600332V